Journal of
Medicinal
Chemistry

Volume 45, Number 13 June 20, 2002

Articles

Structural Differences of Matrix Metalloproteinases with Potential Implications for Inhibitor Selectivity Examined by the GRID/CPCA Approach

Gitte Elgaard Terp,[†] Gabriele Cruciani,[‡] Inge Thøger Christensen,[§] and Flemming Steen Jørgensen*[,†]

Department of Medicinal Chemistry, Royal Danish School of Pharmacy, Universitetsparken 2, DK-2100 Copenhagen, Denmark, Laboratory for Chemometrics, University of Perugia, Via Elce di Sotto 10, I-06123 Perugia, Italy, and Novo Nordisk A/S, Novo Nordisk Park, DK-2760 Måløv, Denmark

Received April 20, 2001

The matrix metalloproteinases (MMPs) are a family of proteolytic enzymes, which have been the focus of a lot of research in recent years because of their involvement in various disease conditions. In this study, structures of 10 enzymes (MMP1, MMP2, MMP3, MMP7, MMP8, MMP9, MMP12, MMP13, MMP14, and MMP20) were examined with the intention of highlighting regions that could be potential sites for obtaining selectivity. For this purpose, the GRID/CPCA approach as implemented in GOLPE was used. Counterions were included to take into account the different electrostatic properties of the proteins, and the GRID calculations were performed, allowing the protein side chains to move in response to interaction with the probes. In the search for selectivity, the MMPs are known to be a very difficult case because the enzymes of this family are very similar. The well-known differences in the S1′ pocket were observed, but in addition, the pockets S3 and S2 called for attention. This is an observation that emphasizes the need for design of inhibitors exploiting the unprimed side of the active site, if possible, in combination with the S1′ site. Despite small differences, a rational usage of the findings described in this work should make it possible to use a combination of the features of the individual enzyme pockets, making most of the MMP enzymes possible targets for selective inhibition. The results suggest the possibility of distinguishing between 8 of the 10 enzymes by this approach.

Introduction

Matrix metalloproteinases (MMPs) belong to a family of zinc- and calcium-dependent endopeptidases denoted metzincins. The MMPs are responsible for degradation of a variety of extracellular matrix components in both normal tissue remodeling and pathological states. They are known to participate in various disease states such as arthritis, cancer, and osteoporosis, which involve degradation of connective tissue.[1] In the diseased states, the activity of the MMPs is not controlled adequately by the normal regulatory mechanisms (expression control, activation control, and inhibition by the tissue inhibitors of metalloproteinases). Presently, at least 22 different human MMPs are known. They can be classified into five different groups (collagenases, stromelysins, gelatinases, membrane-type MMPs, and others) according to location, structural similarity, and substrate preferences. Structures of the catalytic domains of collagenase 1, 2, and 3 (MMP1, MMP8, and MMP13 respectively), stromelysin 1 (MMP3), gelatinase A (MMP2), and matrilysin (MMP7) are available. The

* To whom correspondence should be addressed. Phone: +45 35 30 63 78. Fax: +45 35 30 60 40. E-mail: fsj@dfh.dk.
[†] Royal Danish School of Pharmacy.
[‡] University of Perugia.
[§] Novo Nordisk A/S.

10.1021/jm0109053 CCC: $22.00
Published on Web 05/16/2002

structures of MMPs have been determined either as apoenzymes or proenzymes or with structurally different inhibitors. For MMP2 and MMP3, both structures of the catalytic domain and structures containing the proenzyme part are available. It is observed that the presence of the proenzyme part affects the structure of the catalytic domain remarkably. The proenzymes and the inhibited enzymes are both inactive, while a zinc ion necessary for substrate cleavage is bound to either the proenzyme part or a small zinc-chelating molecule. The zinc-chelating groups most often encountered are carboxylates, hydroxamates, sulfur compounds, and phosphorus compounds. Lately, MMP structures inhibited by the tissue inhibitors of metalloproteinases (TIMPs) have been determined,[2,3] and structures of TIMPs (of which there are four known to date) have been determined independently too.[4,5] However, when the structural properties of the active MMP enzymes are examined, the structures inhibited by TIMPs and the proenzyme structures should be ignored, since observed conformational changes of the MMPs are observed.

MMP Catalytic Domains. The catalytic domains of MMPs are generally very similar with sequence similarities in the range 50−88% and identities in the range 33−79%.[6] The common structural features include three α-helices and a β-sheet consisting of four parallel and one antiparallel strand. The MMPs are zinc- and calcium-dependent, and all known structures contain two zinc ions and between one and three calcium ions. The active site is a cavity spanning the entire enzyme, and it has been shown that a substrate containing at least six amino acids (three on each side of the scissile bond) is required for the proteolytic activity of MMPs; these six amino acids occupy the subsites S3−S3′ (notation according to Schechter and Berger).[7] All MMP structures contain the common sequence motif HExGHxxGxxH where the three histidines coordinate the catalytic zinc ion. The MMPs are homologous enzymes, share a high degree of sequence similarity, and have very similar three-dimensional structures, and therefore, they seem to be obvious targets for homology modeling.[8,9]

MMP Selectivity. Attempts to obtain selectivity among the enzymes have concentrated mostly on the S1′ site where obvious differences between some of the MMP structures are found. The S1′ pockets are surrounded by a loop, which is of different length and amino acid composition in the individual MMPs, and therefore, there is a possibility of exploiting the resulting differences in the structures for selectivity purposes. The S1′ pockets are generally quite large in all the MMPs. However, in the X-ray structure of MMP1, an arginine defines the bottom of the pocket, whereas in MMP7 a tyrosine fulfills this purpose. In both cases this lead to enzymes with small and restricted pockets. It has been reported, though, that flexibility of this part of the structure in some cases could lead to an induced fit upon ligand binding. This is observed in a published X-ray structure of MMP1[10] where the arginine residue moves, making the pocket able to accommodate larger substituents. In all other MMPs considered, this residue is either a leucine or a threonine and the pocket adopts an extended shape. This includes MMP8, although it resembles MMP1 by having an arginine defining the bottom of the S1′ pocket. Considerable effort has been put into exploiting the deep and broad S1′ pocket in MMP3 by using large inhibitor P1′ groups. This could be a way to obtain selectivity for MMP3 over MMP1 and MMP7, which have fairly short S1′ pockets, whereas all other MMPs have a pocket more like MMP3. The S2′ and S3′ subsites are partly solvent-exposed and can accommodate a wide range of functionalities, but differences in the residues surrounding these sites might be used for selectivity purposes. The primed sites of the active site have been described in detail,[11,12] but generally, the unprimed sites have not been examined thoroughly. There are examples, though, that selectivity is obtained by inhibitors binding in these sites.[13,14] This could lead to the conclusion that these sites are more important than previously anticipated when aiming for selectivity, and the examination of this feature is one of the main goals of this study.

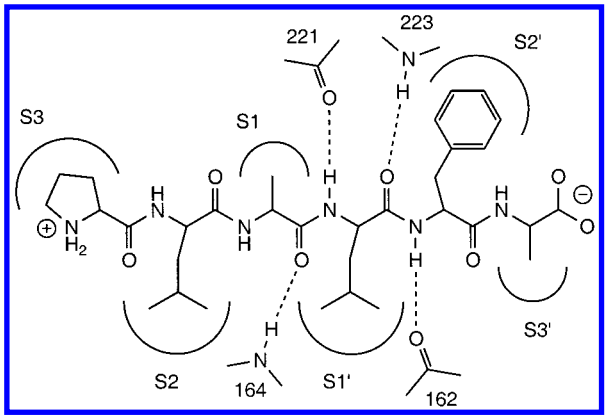

Figure 1. Depiction of possible hydrogen bonds (dotted lines) between a substrate and the MMP backbone.

Inhibitor Binding in MMPs. Most of the known MMP inhibitors are peptidomimetics and exert their function by coordinating to residues in the primed site. They make hydrogen bonds to the backbone of the residues 162(O), 164(N), 221(O), and 223(N) in the enzymes (see Figure 1). These inhibitors frequently occupy the enzyme pockets normally filled by the side chains of natural substrates. Different zinc-binding groups are observed in the inhibited MMP X-ray structures, e.g., hydroxamates, carboxylates, and sulfur compounds. In addition, phosphorus compounds have been widely used as zinc chelators, but no crystal structure of an MMP with a phosphor-containing inhibitor has been published yet. Regarding the strength of the inhibitors, the hydroxamates should intuitively be the best chelating group, since this group has the best coordination geometry and proteolytic properties. This is in accordance with experimental data,[15,16] where carboxylic compounds are seen to be weaker inhibitors, and in addition, the sulfur compounds are even weaker than these. A promising alternative for MMP inhibition is the phosphorus compounds, which have the potential to occupy both sides of the active site, benefiting from interactions in both primed and unprimed subsites,[17−20] which would increase the possibilities of obtaining selective inhibitors.

GRID/CPCA. The GRID/CPCA method has been implemented in GOLPE[21] and can be used for characterization of structural differences that could potentially lead to the design of selective ligands. The method has

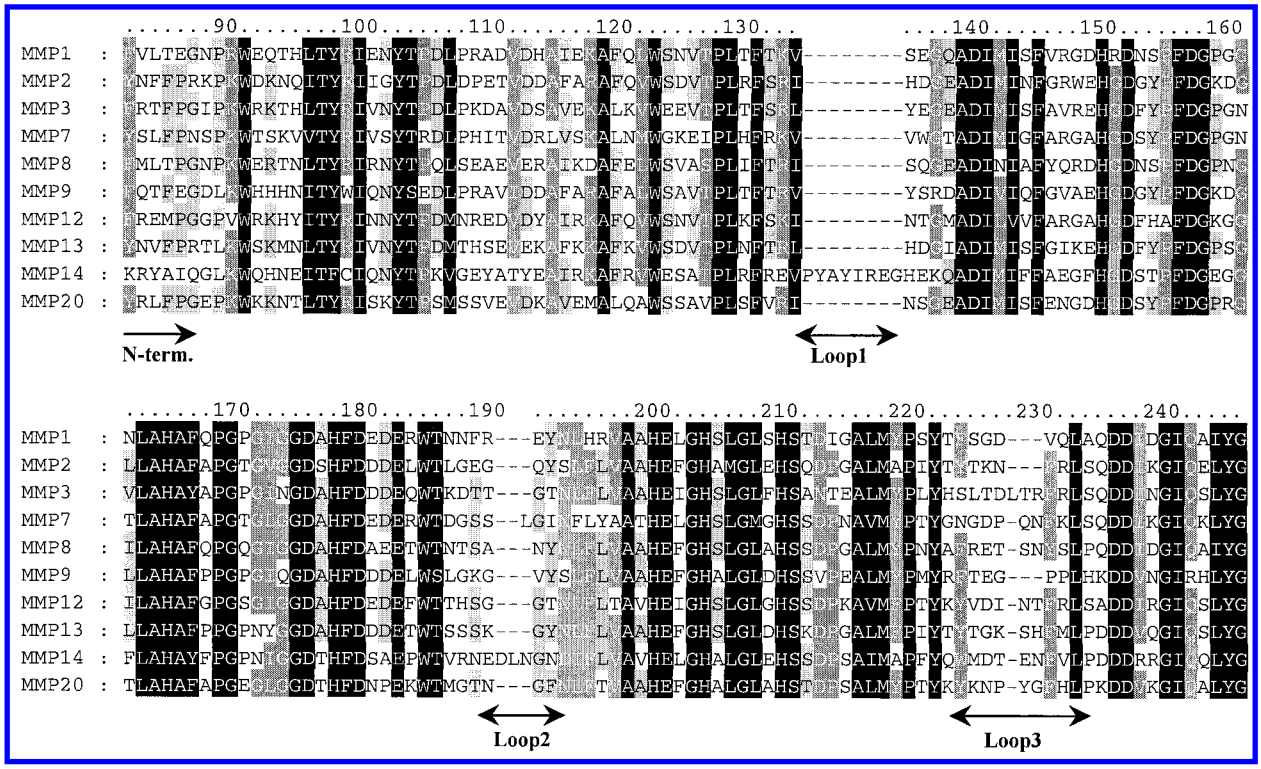

Figure 2. Sequence alignment for the catalytic domain of 10 MMP structures. Numbering is according to the sequence of MMP3. The degree of shading correlates to the amino acid similarity.

Table 1. Overview of GRID Probes Used in the GRID/CPCA Analysis

name	chemical group
DRY	hydrophobic probe
N1	neutral flat NH, e.g., amide
N:	sp^3 N with lone pair, bonded to three heavy atoms
NH=	sp^2 NH with lone pair
N1+	sp^3 amine NH cation, charge of +1
NM3	trimethylammonium cation, charge of +1
O	sp^2 carbonyl oxygen
OH	phenol or carboxy OH
OS	oxygen of sulfone/sulfoxide
O::	sp^2 carboxy oxygen atom

been successfully used to describe and evaluate differences between three serine proteases.[22] The results were compared to available experimental data, and there was good agreement between the observed differences in structure and corresponding inhibitor selectivity. In contrast to CoMFA and related methods[11,23,24] that use a large number of quantitative descriptors to correlate changes in observed biological activity with changes in the chemical structure, GRID/CPCA includes variable selection and is compound-independent.[25] By this method, a few significant variables are extracted from large amounts of redundant information. In addition, the CoMFA method requires prior knowledge of ligand binding data, which is not necessary in the GRID/CPCA approach. This approach enables the usage of enzyme structures and direct comparison of observed features (interactions with GRID probes).

In this paper, 10 MMP structures are characterized by examination of the molecular interaction fields (MIFs) obtained by 10 different GRID probes. The description and analysis of structures were based on the use of GRID, which quantifies the interaction between different probes and the enzymes. The differences were evaluated using the consensus principal component analysis (CPCA) method implemented in GOLPE.[21] This procedure made it possible to evaluate the relative importance of the different probes for selectivity. In addition, the comparison of several different proteins becomes easy to interpret using this procedure. The structure-based design of MMP inhibitors has been a very active research area lately,[26,27] and in the following, we present several structural differences that are of specific interest in the search for selective MMP inhibitors.

Materials and Methods

Amino acid sequences were retrieved from the SWISS-PROT protein sequence data bank.[28,29] The sequences were MMP9 (entry P14780),[30] MMP12 (entry P39900),[31] MMP13 (entry P45452),[32] MMP14 (entry P50281),[33] and MMP20 (entry O60882).[34] The available X-ray structures of human MMP enzymes were retrieved from the RCSB protein data bank.[35] The structures were MMP1 (pdb entry 1HFC),[36] MMP2 (pdb entry 1QIB),[37] MMP3 (pdb entry 1HFS),[38] MMP7 (pdb entry 1MMQ),[39] and MMP8 (pdb entry 1JAP).[40] The sequence alignment was performed using the program ClustalX[41] and revised by minor manual adjustments (see Figure 2). Homology modeling and energy minimization of all structures were performed as described previously.[42] Structures were fitted to each other using the Cα carbon atoms of residues 161−168 and 221−223, which line the active sites. Hydrogens were added by the program GRIN. Counterions were added using MINIM and FILMAP[21] to eliminate large electrostatic differences between the structures. The GRID box dimensions were chosen to encompass all important parts of the active site. The grid spacing was set to 1 Å, and the molecular interaction fields (MIFs) for 10 different GRID probes (see Table 1) were calculated using the GRID program, version 19.[43−46] The MOVE option in GRID was used in order to take side chain flexibility into account.[47] In this way multiple side chain rotamers are considered simultaneously in a single GRID calculation. Statistical evaluation of the obtained fields was performed using the CPCA function implemented in GOLPE.[21]

The data were pretreated, using the region cutout tool in

Table 2. Overview of Favorable Ligand Properties at the Different MMP Subsites, As Revealed from the GRID/CPCA Analysis

	S3	S2	S1	S1′ top	S1′ bottom	S2′	S3′
MMP1	H-bond acceptor			small, neg charged	closed pocket		
MMP2		small, pos charged/H-bond acceptor					
MMP3						polar	polar
MMP7		hydrophobic		small, hydrophobic	closed pocket	polar	polar
MMP8	H-bond acceptor				neg charged		
MMP9							
MMP12		H-bond acceptor		H-bond acceptor	neg charged		polar
MMP13							
MMP14	small H-bond acceptor	small, pos charged/H-bond acceptor			hydrophobic	hydrophobic	polar
MMP20		hydrophobic		H-bond acceptor	neg charged	polar	

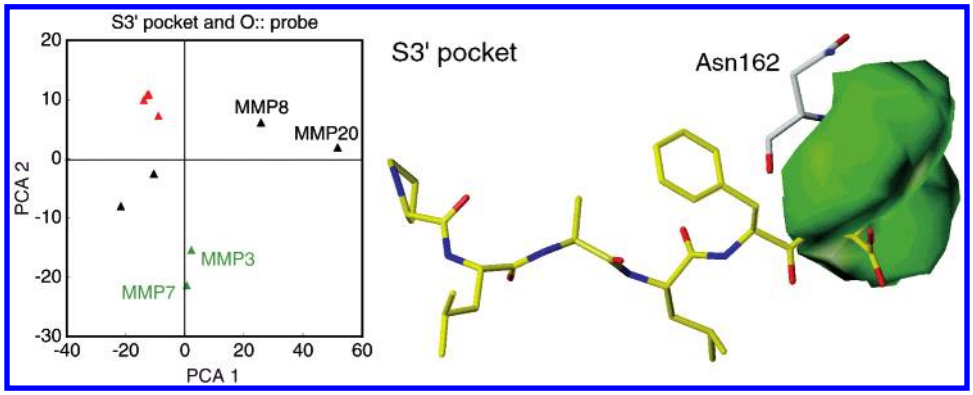

Figure 3. CPCA pseudofield plot (right part) and PCA score plot (left part) for the GRID O:: probe within the S3′ pocket. The field difference in favor of MMP3 and MMP7 (green triangles in the PCA score plot) versus MMP1, MMP2, MMP9, and MMP13 (red triangles) is shown as a green contour. The asparagine in position 162 in MMP3 and MMP7 is shown. The model substrate PLALFA (yellow) is included for illustrative purposes only.

GOLPE. This allowed focusing on specific regions of interest, while regions not important could be left out from the calculations. A model substrate (PLALFA)[42] was used for defining the important regions in the active site, corresponding to the subsites S3−S3′. Each subsite was examined individually, leading to six regions, each with a radius of 4 Å. It was necessary to treat the subsites individually because weak interactions in one region could be obscured by stronger interactions in another region, e.g., from extensive solvent exposure. For the S1′ subsite an additional calculation was performed with the radius set to 7 Å. Region cutout reduces the number of field variables to approximately 1−3% of the original amount. All positive interaction energies were excluded from the data set, and data points with an absolute value smaller than 0.01 or a standard deviation less than 0.1 were set to zero. To take into account the very different interaction energies obtained with the different probes, scaling was performed (block unscaled weights) to make sure that each probe would get the same importance in the model.

Results and Discussion

The 10 MMP structures were evaluated with emphasis on differences and similarities as expressed by interaction energies with different GRID probes. The interpretation of the MIFs became more straightforward by translation of the CPCA loadings into contour plots. The results from the analysis were not included in the interpretation of fields if less than 50% of the variance was explained by the two first components and data were not supported by results from other probes. In the following, each subsite is described individually, and an overview of the obtained results is presented in Table 2.

S3′ Pocket. In all MMPs, the S3′ pockets are relatively neutral in nature and are partly solvent-exposed. This is seen by the fact that the dry probe does not distinguish between any of the proteins. However, MMP3, MMP7, MMP12, and MMP14 display favorable interactions with a carboxy oxygen atom probe, with MMP3 and MMP7 displaying the best interactions. This is partly due to a more restricted pocket in the other MMPs. The pocket size is highly dependent on the residue at position 193, which is located in loop 2 (see Figure 2). MMP1, MMP2, MMP8, MMP9, MMP13, and MMP20 contain a tyrosine/phenylalanine residue at this position and have a smaller pocket than the structures containing threonine (MMP3 and MMP12), isoleucine (MMP7), or asparagine (MMP14). The more favorable interaction with MMP3 and MMP7 could be explained by the presence of an asparagine in position 162 in these two enzymes (glycine in all other proteins) (see Figure 3). With the N1 probe (resembling an amide nitrogen), MMP3, MMP7, MMP8, and MMP14 could be distinguished from the other proteins, again with MMP3 and MMP7 clustering together. The interactions with these four MMPs are more favorable than with the remaining MMPs, which must be a consequence of asparagines surrounding this site at different positions (Asn162 in MMP3 and MMP7, Asn161 in MMP8, and Asn193 in MMP14). The same feature is observed with the positively charged probes (N1+ and NM3). Because of the solvent exposure, the observed differences might be of less value. There is a possibility, though, that interactions of MMP3, MMP7, MMP12, and MMP14 with polar probes would distinguish these MMPs from the remaining.

S2′ Pocket. The S2′ pocket is very similar in all structures because it is partly solvent-exposed, although the size of the pocket is affected by the residues in positions 162 and 163. MMP14 is clearly favored by the dry probe because the site is lined by a phenylalanine (Phe163) (see Figure 4). All polar probes interact more favorably with MMP3, MMP7, and MMP20 than with

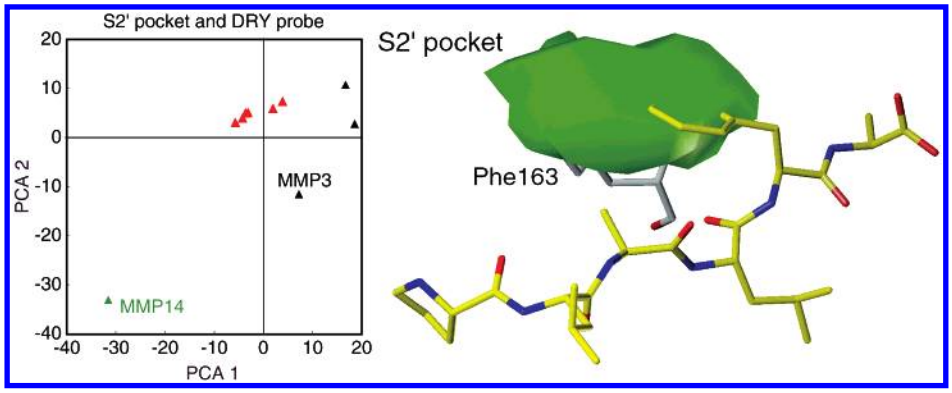

Figure 4. CPCA pseudofield plot (right part) and PCA score plot (left part) for the GRID dry probe within the S2′ pocket. The field difference in favor of MMP14 (green triangle in the PCA score plot) versus MMP1, MMP2, MMP8, MMP9, MMP12, and MMP13 (red triangles) is shown as a green contour. The phenylalanine in position 163 in MMP14 is shown. The model substrate PLALFA (yellow) is included for illustrative purposes only.

the remaining proteins. This might simply be a consequence of the pocket being more solvent-exposed but could also be associated with the presence of a threonine in position 163 in MMP7 and MMP20 and an asparagine in position 162 of MMP3 and MMP7, making polar interactions more favorable in these three MMPs. With a positively charged probe, it is possible to distinguish clearly between MMP20 and MMP3/MMP7, since MMP3 and MMP7 interact much more strongly with the positively charged probe. However, the solvent exposure of the S2′ site makes it of less value for selective inhibition.

S1′ Pocket. The S1′ pocket is surrounded by loop 3 (see Figure 2), which is of different length in the enzymes, and consequently, different spatial positions of the amino acids are observed. Independent of variations in size and shape, the S1′ pocket is often characterized as a hydrophobic pocket in all MMPs. The most pronounced difference between the enzymes at this site is the residue in position 197, which is a leucine in all enzymes except for MMP1, MMP7, and MMP20, where an arginine, a tyrosine, and a threonine is present, respectively. The S1′ pocket is broad and elongated in all structures except for MMP1 and MMP7, and this is in accordance with peptide cleavage studies on model peptides.[48−50] However, the flexibility of this loop opens up possibilities for accommodating ligands by an induced-fit mechanism, and this could not be predicted from the rigid enzyme structures. If the protein side chains are allowed to move when interacting with the GRID probes, a prediction of this feature could be performed to some extent. Calculations of the solvent-accessible surfaces of MMP1 and MMP7 (with and without usage of the "MOVE" option in GRID) show that the pocket in MMP1 is able to change its shape, making it accessible to more bulky substituents (see Figure 5). However, the pocket is still not as wide as the pockets of the remaining proteins. In contrast, the GRID calculations indicate that MMP7 does not have the possibility of creating an open S1′ pocket like the one observed in MMP1 (see Figure 5). However, these calculations could only illustrate side chain flexibility and cannot handle main chain movements. Because of sequence variation and nonsimilar backbone conformations around the S1′ pocket in the enzymes, a number of other differences are observed that lead to very different pocket shapes. Therefore, it is not surprising that much effort has been put into exploring this site for selectivity purposes.

Interaction with the dry probe is most favorable for MMP7 at the top of the pocket due to the possibility of interaction with Tyr197. Obviously, this will distinguish MMP7 from all other proteins. MMP1 and MMP7 are distinguished by interacting less favorably with the N1 probe (neutral flat NH) compared with the other enzymes. This is due to the closed pocket in these enzymes. Favorable interactions occur between the N: probe (sp^3 nitrogen with lone pair bonded to three heavy atoms) and MMP8, MMP12, and MMP20, the interactions with MMP12 and MMP20 being most favorable. This is due to Thr198 in MMP12 and Thr197 in MMP20. This feature could also be exploited with probes able to accept hydrogen bonds, e.g., OH (phenol or carboxy OH)and OS (oxygen of sulfone/sulfoxide), where the interactions with MMP12 and MMP20 are most favorable (see Figure 6). Actually, this feature is observed with all polar probes, and it should be possible to use these distinct differences of MMP12 and MMP20 for selectivity purposes, since the other proteins have hydrophobic residues at these positions. An exception is MMP1, which has an arginine in position 197, but this protein is, as previously mentioned, distinguished by its closed pocket. In conclusion, MMP1 and MMP7 could be targeted selectively because of their closed pockets, while the hydrogen bond accepting properties of MMP12 and MMP20 could be used to distinguish these two MMPs from the remaining.

Because the S1′ pockets in most cases are wide and elongated, it could be anticipated that differences further down the pocket could be exploited for selectivity purposes. This was examined by extending the region of interest to 7 Å, and in fact it was found that several of the proteins have features in this region, which might be used for selectivity purposes. As previously mentioned, inspection of MMP1 and MMP7 in this respect is meaningless because these pockets are closed.

At the bottom of the S1′ pocket, MMP14 shows favorable interactions with the dry probe due to the presence of Met237 at the bottom of the pocket. Interactions with OH and OS probes are most favorable for MMP8, MMP12, and MMP20 because of the possibility of interaction with positively charged residues (lysines and arginines at positions 224 and 226, respectively). MMP2, MMP3, MMP9, and MMP13 seem to have

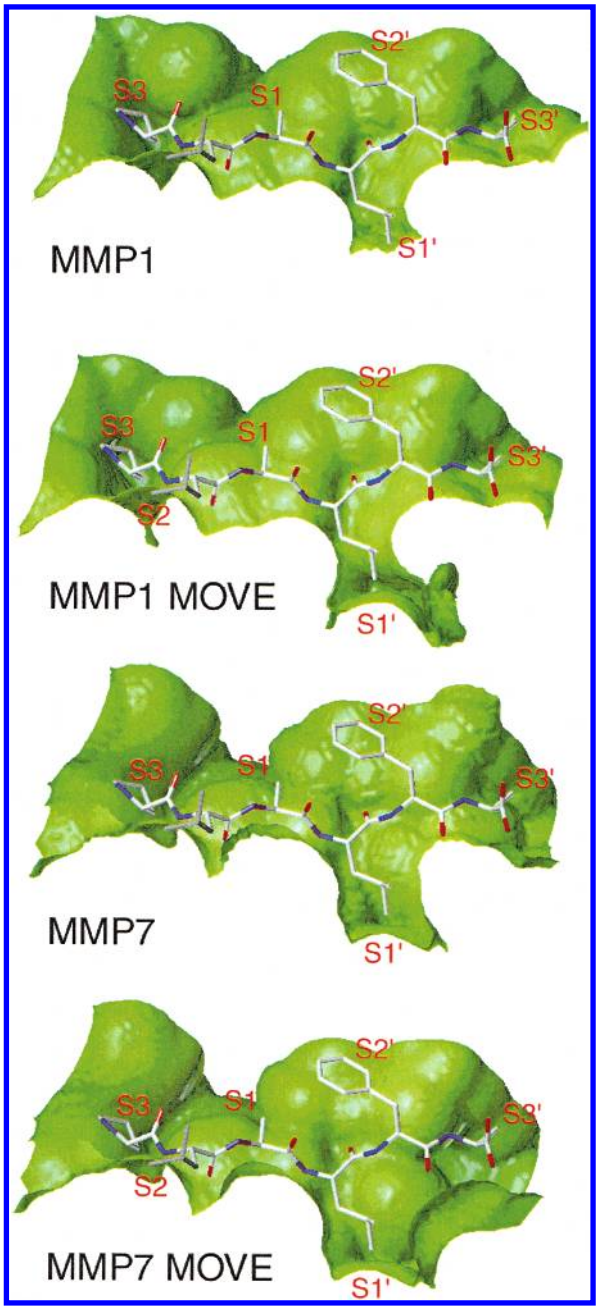

Figure 5. Solvent-accessible surfaces of MMP1 and MMP7. The left part shows GRID contours when rigid enzyme structures are encountered, while the right part is the result of calculations, where the enzyme side chains are allowed to move in response to interaction with the water probe. The S1′ pocket of MMP1 is shown to change considerably and to adopt a more extended shape. Contours are depicted at 0 kcal/mol. The model substrate PLALFA is included for illustrative purposes only.

totally open pockets and are not displaying any significant interactions. Interestingly, it has been possible to derive inhibitors that show some selectivity between MMP9 and MMP13, utilizing differences in the S1′ pocket.[51,52] Since side chain flexibility is considered in the GRID/CPCA approach, it suggests that the inhibitors capable of distinguishing between the two enzymes induce backbone conformational changes. MMP1, MMP7, MMP14, and MMP20 display unfavorable interactions with positively charged probes because of closed pockets. Similarly, interactions between positively charged probes and the bottom of the pockets in MMP8 and MMP12 are unfavorable because of positively charged residues at this position in these enzymes. MMP8, MMP12, and MMP20 could be distinguished by probes interacting with positively charged residues at the bottom of the pockets, while MMP14 interacts favorably with hydrophobic probes.

S1 Pocket. Regarding the S1 pocket, Phe163 causes a decrease in the size of the pocket in MMP14. In MMP1 an asparagine is occupying this position, making the site less hydrophobic than in the other structures, which contain a leucine, valine, threonine, or isoleucine at this position. However, no significant differences could be observed at this site.

S2 Pocket. MMP12 is clearly distinguished from the other enzymes with all GRID probes at the S2 pocket, but this may be a result of the extensive solvent exposure of this site in that particular enzyme. Arg84 and Met86 are surrounding this pocket, but both side chains are able to move, making the pocket very wide and solvent-exposed. The interactions of the dry probe with MMP7 and MMP20 are more favorable than with the remaining proteins. This is due to the residue in position 210, which varies considerably in the MMPs and is located in such a way that it may affect the shape and properties of the S2 pocket. In MMP7 and MMP20, very small and hydrophobic residues are encountered in position 210 (glycine/alanine). This is also the case in MMP8 (alanine), but the presence of Gln169 in MMP8 makes the steric hindrance more pronounced. With the N1 probe, the interactions with MMP2 and MMP14 are much more favorable than with the other proteins (including MMP12). This is due to Glu210 in these two enzymes, which is capable of interacting favorably with this probe. MMP12 also interacts with this probe, but this is not due to the residue in position 210 but to positive interaction with the methionine in position 86. In that respect, it is possible to distinguish MMP12 from the other enzymes, and in addition to this, MMP2 and MMP14 could be addressed selectively by choosing substituents that interact favorably with Glu210 (see Figure 7). With the N-containing probes with lone pairs (N: and NH═), interaction with MMP2 and MMP14 is most favorable with the probe that is not sterically demanding (NH═), while the interactions are unfavorable with the more sterically demanding probe (N:). This is a direct result of the ability of the glutamic acid to interact favorably with these probes and the size of this residue. MMP12 still interacts favorably with both these probes because of its more open site. MMP2 and MMP14 interact very well with the positively charged probes (N1+ and NM3), and this clearly distinguishes these MMPs from the remaining. This effect is most pronounced with the N1+ probe, since the larger probe (NM3) encounters some steric hindrance. MMP12 also interacts very well because of the presence of the methionine. The interaction with a carbonyl oxygen is very favorable for MMP12 due to Arg84, whereas this interaction is most unfavorable for MMP2 and MMP14 with the glutamic acid in position 210. With the OH and OS probes, MMP2, MMP12, and MMP14 are distinguished from the other proteins. MMP2 and MMP14 interact very well with the OH probe (even better than MMP12), whereas with the OS

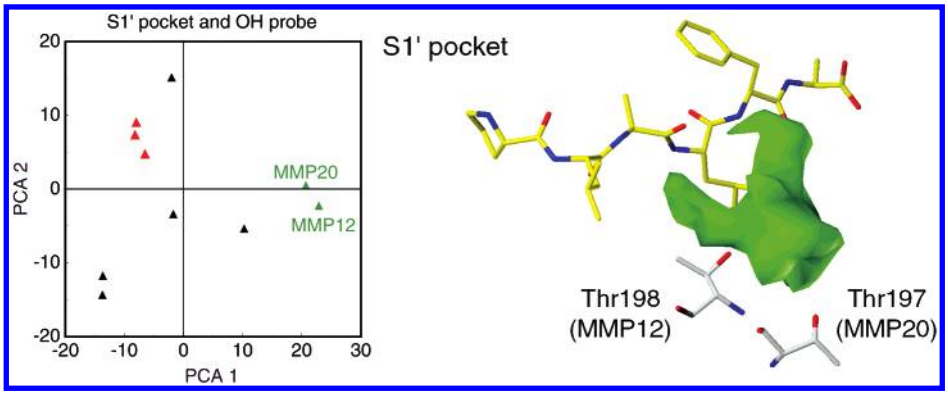

Figure 6. CPCA pseudofield plot (right part) and PCA score plot (left part) for the GRID OH probe within the S1′ pocket. The field difference in favor of MMP12 and MMP20 (green triangles in the PCA score plot) versus MMP2, MMP9, and MMP13 (red triangles) is shown as a green contour. The threonines lining the pockets in MMP12 and MMP20 are shown. The model substrate PLALFA (yellow) is included for illustrative purposes only.

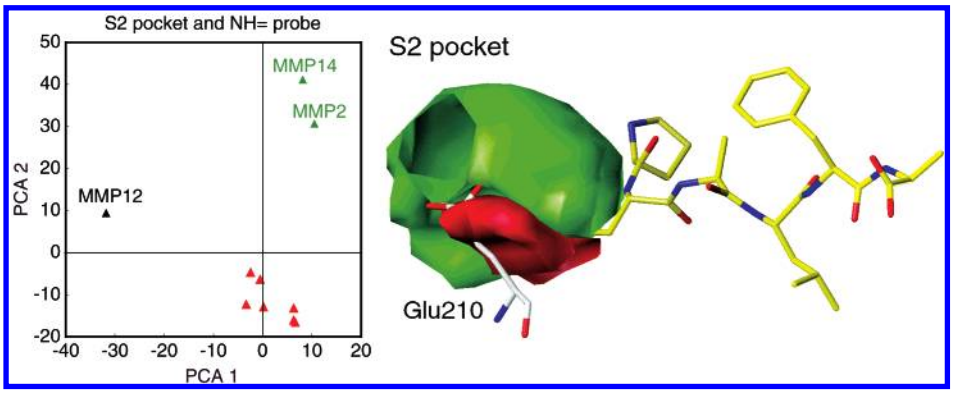

Figure 7. CPCA pseudofield plot (left right part) and PCA score plot (left part) for the GRID N1+ probe within the S2 pocket. The field difference in favor of MMP2 and MMP14 (green triangles in the PCA score plot) versus MMP1, MMP3, MMP7, MMP8, MMP9, MMP13, and MMP20 (red triangles) is shown as a green contour. A glutamic acid in MMP2 and MMP14 is responsible for the positive interactions with the N1+ probe, but because of its size, this residue also implies nonfavorable interactions (red contour). The model substrate PLALFA (yellow) is included for illustrative purposes only.

probe, the sterical hindrance makes the differentiation between the proteins less pronounced.

The shape of the S2 pocket is very much dependent on the N-terminal amino acids. In structures where a proline occupies position 87, the residue at position 86 may affect the pocket size considerably. This is the case in MMP2, MMP3, MMP7, MMP8, MMP12, MMP13, and MMP20. The phenylalanine at position 86 leads to quite small and hydrophobic pockets in the structures of MMP2, MMP3, MMP7, MMP13, and MMP20. In MMP8 and MMP12, position 86 is occupied by a threonine and methionine, respectively, and the pocket is bigger in these two structures. In addition, the residue in position 84 can affect the pocket when a proline is present in position 87. A more positively charged pocket is found in MMP3, MMP12, and MMP20 due to an arginine in position 84. This is in contrast to MMP14, which also contains Arg84, but because of the absence of a proline in position 87, this arginine is positioned differently and does not affect the properties of the S2 pocket. In structures where a proline does not occupy position 87, the N-terminal of the enzyme adopts another conformation and does not affect the size or properties of the S2 pocket. In these enzymes (MMP1, MMP9, and MMP14), the S2 pocket is mainly defined by the residue at position 169. In MMP9 a proline occupies this position and leads to a relatively big hydrophobic pocket, whereas in MMP1 a glutamine reduces the size and hydrophobicity of the pocket. In MMP14 a phenylalanine is located at this site, leading to a small and hydrophobic pocket. MMP7 and MMP20 could be distinguished because these MMPs display favorable interactions with hydrophobic probes. MMP12 requires a hydrogen bond acceptor at the P2 position, which also is the case for MMP2 and MMP14. In these two enzymes, there is also a preference for small, positively charged substituents.

S3 Pocket. In the S3 pocket, the dry probe interacts better with MMP2, MMP3, MMP7, MMP9, MMP12, MMP13, and MMP20 than with MMP1, MMP8 and MMP14. This is due to the residue in position 155, which influences the pocket size, and in structures where a tyrosine (MMP2, MMP3, MMP7, MMP9, MMP13, and MMP20) or a histidine (MMP12) occupies this position, the pocket is smaller than in structures with serine (MMP1 and MMP8) or threonine (MMP14). In all structures, the residue in position 168 is either a phenylalanine or a tyrosine, which leads to restriction of the pocket size and creation of a hydrophobic environment.

The interactions with the N1 probe are most favorable for MMP1 and MMP8. The interactions with MMP14 are also better than the interactions with the remaining MMPs, but because of steric hindrance, this interaction is not as strong as for MMP1 and MMP8 with a serine in position 155. This picture is also observed for the N-containing probes containing lone pairs (N: and NH═). Not surprisingly, with the charged probes, the interactions with MMP1, MMP8, and MMP14 are better

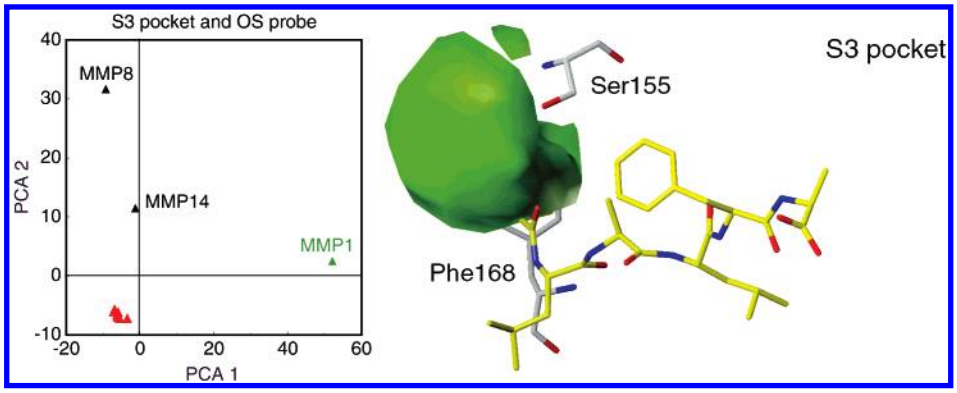

Figure 8. CPCA pseudofield plot (right part) and PCA score plot (left part) for the GRID OS probe within the S3 pocket. The field difference in favor of MMP1 (green triangle in the PCA score plot) versus MMP2, MMP3, MMP7, MMP9, MMP12, MMP13, and MMP20 (red triangles) is shown as a green contour (similar results were obtained for MMP8 and MMP14). The serine residue in MMP1, able to donate hydrogen bonds, is shown. The model substrate PLALFA (yellow) is included for illustrative purposes only.

than the interaction with the other MMPs. The oxygen-containing probes, including the probes capable of making hydrogen bonds to the serine and threonine residues, interact better with MMP1, MMP8, and MMP14 than with the remaining MMPs (see Figure 8). Therefore, it seems possible to distinguish these three MMPs from the others, using the features of the S3 pocket. In addition, MMP1 and MMP8 might also be distinguished from MMP14 by use of more sterically demanding, polar substituents at this site.

Inhibitors. Because of the obvious therapeutic potential, many pharmaceutical companies have worked intensively to develop either broad-spectrum or selective MMP inhibitors. Originally, most inhibitors were peptidomimetic substrate analogues, but because the structural knowledge on MMP has increased, several non-peptidic inhibitors have been reported.[27,53]

In the majority of the published inhibitors, selectivity is obtained by the P1′ substituent. The difference in the size and shape of the S1′ subsite has been utilized to design several series of structurally diverse MMP3 inhibitors.[27] Our GRID/CPCA calculations confirmed this, but they also showed that different types of interactions in the S1′ pocket could be used to distinguish between several of the MMPs (cf. Table 2).

The S2′ and S3′ subsites are relatively solvent-exposed, and a wide range of substituents are tolerated in these subsites. In previously reported reviews on SAR of MMP inhibitors, it was concluded that these sites do not play a dominant role in inhibitor binding, and thus, they would be difficult to use for optimization of selectivity.[27,53] Because peptides generally suffer from unfavorable pharmacokinetic properties, substituents in these subsites have been used to optimize oral bioavailability and solubility.[38,54]

The GRID/CPCA calculations did not reveal any significant difference between the different MMPs in the S1 subsite. Therefore, it was predicted that selectivity is not likely to be achieved from interactions in this pocket. These findings are in agreement with literature data. Although selective inhibitors exploring the S1 pocket have been reported, the selectivity has been obtained by benefiting from differences in other subsites.[55]

Reiter et al.[13] reported that for a series of phosphinate inhibitors it is possible to use the differences in the hydrophobicity of the S2 subsites of MMP1, MMP3, and MMP13 to obtain selectivity between the enzymes. However, these differences where not demonstrated in the GRID/CPCA calculations.

In a series of thiadiazole-containing MMP inhibitors, nanomolar activity at MMP3 was obtained by optimizing interactions in the S3 subsite.[14,56] The most potent inhibitor was shown by X-ray crystallography to form $\pi-\pi$ interactions with the tyrosine in position 155.[14] While inhibitors of this class were moderately potent at MMP2 (~1 mM), they were totally inactive at MMP1. This is in agreement with the GRID/CPCA calculations, which distinguish between MMP1/MMP8/MMP14 and the remaining MMPs (cf. Table 2). Because of the presence of a serine or threonine in the S3 subsite, it is predicted that MMP1/MMP8/MMP14 selectivity could be obtained by placing a hydrogen bond acceptor in the P3 position.

Conclusion

The GRID/CPCA approach was used successfully to examine and highlight differences in matrix metalloproteinases. Especially at the S3, S2, and S1′ sites, there are considerable differences among the structures, and these sites are predicted to be very important in the design of selective ligands. Even though the most obvious differences are observed at the S1′ site, it must be concluded that there are other possibilities for obtaining selectivity by using the differences observed at the unprimed sites. In fact, the possibility of obtaining selectivity here might be of utmost importance, since the primed sites (with the exception of S1′) are quite solvent-exposed. The described differences in the S3 and S2 pockets should make it possible to distinguish between several of the enzymes, and in combination with the S1′ pocket, there are plenty of possibilities to obtain selective inhibitors. The importance of having a tool to display these differences in an easily interpretable way has been shown to be very valuable. Combining the present findings in a rational way should make it possible to develop selective inhibitors for most of the MMPs, and the present combination of methods is therefore anticipated to have wide potential in structure-based ligand design.

Acknowledgment. We are grateful to Tripos Associates for support in connection with our use of SYBYL.

References

(1) Shapiro, S. D. Matrix Metalloproteinase Degradation of Extracellular Matrix: Biological Consequences. *Curr. Opin. Cell Biol.* **1998**, *10*, 602−608.

(2) Gomis-Rüth, F.-X.; Maskos, K.; Betz, M.; Bergner, A.; Huber, R.; Suzuki, K.; Yoshida, N.; Nagase, H.; Brew, K.; Bourenkov, G. P.; Bartunik, H.; Bode, W. Mechanism of Inhibition of the Human Matrix Metalloproteinase Stromelysin-1 by TIMP-1. *Nature* **1997**, *389*, 77−81.

(3) Fernandez-Catalan, C.; Bode, W.; Huber, R.; Turk, D.; Calvete, J. J.; Lichte, A.; Tschesche, H.; Maskos, K. Crystal Structure of the Complex Formed by the Membrane Type 1-Matrix Metalloproteinase with the Tissue Inhibitor of Metalloproteinases-2, the Soluble Progelatinase A Receptor. *EMBO J.* **1998**, *17*, 5238−5248.

(4) Muskett, F. W.; Frenkiel, T. A.; Feeney, J.; Freedman, R. B.; Carr, M. D.; Williamson, R. A. High Resolution Structure of the N-Terminal Domain of Tissue Inhibitor of Metalloproteinases-2 and Characterization of Its Interaction Site with Matrix Metalloproteinase-3. *J. Biol. Chem.* **1998**, *273*, 21736−21743.

(5) Tuuttila, A.; Morgunova, E.; Bergmann, U.; Lindquist, Y.; Maskos, K.; Fernandez-Catalan, C.; Bode, W.; Tryggvason, K.; Schneider, G. Three-Dimensional Structure of Human Tissue Inhibitor of Metalloproteinases-2 at 2.1 Å Resolution. *J. Mol. Biol.* **1998**, *284*, 1133−1140.

(6) Sang, Q. A.; Douglas, D. A. Computational Sequence Analysis of Matrix Metalloproteinases. *J. Protein Chem.* **1996**, *15*, 137−160.

(7) Schechter, I.; Berger, A. On the Size of the Active Site in Proteases. I. Papain. *Biochem. Biophys. Res. Commun.* **1967**, *27*, 157−162.

(8) Massova, I.; Kotra, L. P.; Fridman, R.; Mobashery, S. Matrix Metalloproteinases: Structures, Evolution, and Diversification. *FASEB J.* **1998**, *12*, 1075−1095.

(9) Greer, J. Comparative Modeling Methods: Application to the Family of the Mammalian Serine Proteases. *Proteins* **1990**, *7*, 317−334.

(10) Lovejoy, B.; Welch, A. R.; Carr, S.; Luong, C.; Broka, C.; Hendricks, R. T.; Campbell, J. A.; Walker, K. A. M.; Martin, R.; Van Wart, H.; Browner, M. F. Crystal Structures of MMP-1 and -13 Reveal the Structural Basis for Selectivity of Collagenase Inhibitors. *Nat. Struct. Biol.* **1999**, *6*, 217−221.

(11) Matter, H.; Schwab, W. Affinity and Selectivity of Matrix Metalloproteinase Inhibitors: A Chemometrical Study from the Perspective of Ligands and Proteins. *J. Med. Chem.* **1999**, *42*, 4506−4523.

(12) Borkakoti, N. Structural Studies of Matrix Metalloproteinases. *J. Mol. Med.* **2000**, *78*, 261−268.

(13) Reiter, L. A.; Rizzi, J. P.; Pandit, J.; Lasut, M. J.; McGahee, S. M.; Parikh, V. D.; Blake, J. F.; Danley, D. E.; Laird, E. R.; Lopez-Anaya, A.; Lopresti-Morrow, L. L.; Mansour, M. N.; Martinelli, G. J.; Mitchell, P. G.; Owens, B. S.; Pauly, T. A.; Reeves, L. M.; Schulte, G. K.; Yocum, S. A. Inhibition of MMP-1 and MMP-13 with Phosphinic Acids That Exploit Binding in the S2 Pocket. *Bioorg. Med. Chem. Lett.* **1999**, *9*, 127−132.

(14) Finzel, B. C.; Baldwin, E. T.; Bryant, G. L., Jr.; Hess, G. F.; Wilks, J. W.; Trepod, C. M.; Mott, J. E.; Marshall, V. P.; Petzold, G. L.; Poorman, R. A.; O'Sullivan, T. J.; Schostarez, H. J.; Mitchell, M. A. Structural Characterizations of Nonpeptidic Thiadiazole Inhibitors of Matrix Metalloproteinases Reveal the Basis for Stromelysin Selectivity. *Protein Sci.* **1998**, *7*, 2118−2126.

(15) Porter, J. R.; Beeley, N. R. A.; Boyce, B. A.; Mason, B.; Millican, A.; Millar, K.; Leonard, J.; Morphy, J. R.; O'Connell, J. P. Potent and Selective Inhibitors of Gelatinase-A 1. Hydroxamic Acid Derivatives. *Bioorg. Med. Chem. Lett.* **1994**, *4*, 2741−2746.

(16) Morphy, J. R.; Beeley, N. R. A.; Boyce, B. A.; Leonard, J.; Mason, B.; Millican, A.; Millar, K.; O'Connell, J. P.; Porter, J. Potent and Selective Inhibitors of Gelatinase-A 2. Carboxylic and Phosphonic Acid Derivatives. *Bioorg. Med. Chem. Lett.* **1994**, *4*, 2747−2752.

(17) Caldwell, C. G.; Sahoo, S. P.; Polo, S. A.; Eversole, R. R.; Lanza, T. J.; Mills, S. G.; Niedzwiecki, L. M.; Izquierdo-Martin, M.; Chang, B. C.; Harrison, R. K.; Kuo, D. W.; Lin, T.-Y.; Stein, R. L.; Durette, P. L.; Hagmann, W. K. Phosphinic Acid Inhibitors of Matrix Metalloproteinases. *Bioorg. Med. Chem. Lett.* **1996**, *6*, 323−328.

(18) Yiotakis, A.; Lecoq, A.; Vassiliou, S.; Raynal, I.; Cuniasse, P.; Dive, V. Cyclic Peptides with a Phosphinic Bond as Potent Inhibitors of a Zinc Bacterial Collagenase. *J. Med. Chem.* **1994**, *37*, 2713−2720.

(19) Jirácek, J.; Yiotakis, A.; Vincent, B.; Lecoq, A.; Nicolaou, A.; Checler, F.; Dive, V. Development of Highly Potent and Selective Phosphinic Peptide Inhibitors of Zinc Endopeptidase 24-15 Using Combinatorial Chemistry. *J. Biol. Chem.* **1995**, *270*, 21701−21706.

(20) Pikul, S.; McDow Dunham, K. L.; Almstead, N. G.; De, B.; Natchus, M. G.; Anastasio, M. V.; McPhail, S. J.; Snider, C. E.; Taiwo, Y. O.; Chen, L.; Dunaway, C. M.; Gu, F.; Mieling, G. E. Design and Synthesis of Phosphinamide-Based Hydroxamic Acids as Inhibitors of Matrix Metalloproteinases. *J. Med. Chem.* **1999**, *42*, 87−94.

(21) Molecular Discovery Ltd., Perugia, Italy.

(22) Kastenholz, M. A.; Pastor, M.; Cruciani, G.; Haaksma, E. E.; Fox, T. GRID/CPCA: A New Computational Tool To Design Selective Ligands. *J. Med. Chem.* **2000**, *43*, 3033−3044.

(23) Matter, H.; Schwab, W.; Barbier, D.; Billen, G.; Haase, B.; Neises, B.; Schudok, M.; Thorwart, W.; Schreuder, H.; Brachvogel, V.; Lönze, P.; Weithmann, K. U. Quantitative Structure−Activity Relationship of Human Neutrophil Collagenase (MMP-8) Inhibitors Using Comparative Molecular Field Analysis and X-ray Structure Analysis. *J. Med. Chem.* **1999**, *42*, 1908−1920.

(24) Klebe, G.; Abraham, U.; Mietzner, T. Molecular Similarity Indices in a Comparative Analysis (CoMSIA) of Drug Molecules To Correlate and Predict Their Biological Activity. *J. Med. Chem.* **1994**, *37*, 4130−4146.

(25) Cruciani, G.; Watson, K. A. Comparative Molecular Field Analysis Using GRID Force-Field and GOLPE Variable Selection Methods in a Study of Inhibitors of Glycogen Phosphorylase b. *J. Med. Chem.* **1994**, *37*, 2589−2601.

(26) Zask, A.; Levin, J. I.; Killar, L. M.; Skotnicki, J. S. Inhibition of Matrix Metalloproteinases: Structure Based Design. *Curr. Pharm. Des.* **1996**, *2*, 624−661.

(27) Whittaker, M.; Floyd, C. D.; Brown, P.; Gearing, A. J. H. Design and Therapeutic Application of Matrix Metalloproteinase Inhibitors. *Chem. Rev.* **1999**, *99*, 2735−2776.

(28) Bairoch, A.; Apweiler, R. The SWISS-PROT Protein Sequence Database: Its Relevance to Human Molecular Medical Research. *J. Mol. Med.* **1997**, *75*, 312−316.

(29) Bairoch, A.; Apweiler, R. The SWISS-PROT Protein Sequence Data Bank and Its Supplement TrEMBL in 1999. *Nucleic Acids Res.* **1999**, *27*, 49−54.

(30) Wilhelm, S. M.; Collier, I. E.; Marmer, B. L.; Eisen, A. Z.; Grant, G. A.; Goldberg, G. I. SV40-Transformed Human Lung Fibroblasts Secrete a 92-KDa Type IV Collagenase Which Is Identical to That Secreted by Normal Human Macrophages. *J. Biol. Chem.* **1989**, *264*, 17213−17221.

(31) Shapiro, S. D.; Kobayashi, D. K.; Ley, T. J. Cloning and Characterization of a Unique Elastolytic Metalloproteinase Produced by Human Alveolar Macrophages. *J. Biol. Chem.* **1993**, *268*, 23824−23829.

(32) Freije, J. M.; Diez-Itza, I.; Balbin, M.; Sanchez, L. M.; Blasco, R.; Tolivia, J.; Lopez-Otin, C. Molecular Cloning and Expression of Collagenase-3, a Novel Human Matrix Metalloproteinase Produced by Breast Carcinomas. *J. Biol. Chem.* **1994**, *269*, 16766−16773.

(33) Will, H.; Hinzmann, B. CDNA Sequence and MRNA Tissue Distribution of a Novel Human Matrix Metalloproteinase with a Potential Transmembrane Segment. *Eur. J. Biochem.* **1995**, *231*, 602−608.

(34) Llano, E.; Pendas, A. M.; Knauper, V.; Sorsa, T.; Salo, T.; Salido, E.; Murphy, G.; Simmer, J. P.; Bartlett, J. D.; Lopez-Otin, C. Identification and Structural and Functional Characterization of Human Enamelysin (MMP-20). *Biochemistry* **1997**, *36*, 15101−15108.

(35) Bernstein, F. C.; Koetzle, T. F.; Williams, G. J.; Meyer, E. E., Jr.; Brice, M. D.; Rodgers, J. R.; Kennard, O.; Shimanouchi, T.; Tasumi, M. The Protein Data Bank: A Computer-Based Archival File for Macromolecular Structures. *J. Mol. Biol.* **1977**, *112*, 535−542.

(36) Spurlino, J. C.; Smallwood, A. M.; Carlton, D. D.; Banks, T. M.; Vavra, K. J.; Johnson, J. S.; Cook, E. R.; Falvo, J.; Wahl, R. C.; Pulvino, T. A.; Wendoloski, J. J.; Smith, D. L. 1.56 Å Structure of Mature Truncated Human Fibroblast Collagenase. *Proteins* **1994**, *19*, 98−109.

(37) Dhanaraj, V.; Williams, M. G.; Ye, Q.-Z.; Molina, F.; Johnson, L. L.; Ortwine, D. F.; Pavlovsky, A.; Rubin, J. R.; Skeean, R. W.; White, A. D.; Humblet, C.; Hupe, D. J.; Blundell, T. L. X-Ray Structure of Gelatinase A Catalytic Domain Complexed with a Hydroxamate Inhibitor. *Croat. Chem. Acta* **1999**, *72*, 575−591.

(38) Esser, C. K.; Bugianesi, R. L.; Caldwell, C. G.; Chapman, K. T.; Durette, P. L.; Girotra, N. N.; Kopka, I. E.; Lanza, T. J.; Levorse, D. A.; MacCoss, M.; Owens, K. A.; Ponpipom, M. M.; Simeone, J. P.; Harrison, R. K.; Niedzwiecki, L.; Becker, J. W.; Marcy, A. I.; Axel, M. G.; Christen, A. J.; McDonnell, J.; Moore, V. L.; Olszewski, J. M.; Saphos, C.; Visco, D. M.; Shen, F.; Colletti, A.; Krieter, P. A.; Hagmann, W. K. Inhibition of Stromelysin-1 (MMP-3) by P1′-Biphenylylethyl Carboxyalkyl Dipeptides. *J. Med. Chem.* **1997**, *40*, 1026−1040.

(39) Browner, M. F.; Smith, W. W.; Castelhano, A. L. Matrilysin-Inhibitor Complexes: Common Themes among Metalloproteases. *Biochemistry* **1995**, *34*, 6602−6610.
(40) Bode, W.; Reinemer, P.; Huber, R.; Kleine, T.; Schnierer, S.; Tschesche, H. The X-Ray Crystal Structure of the Catalytic Domain of Human Neutrophil Collagenase Inhibited by a Substrate Analogue Reveals the Essentials for Catalysis and Specificity. *EMBO J.* **1994**, *13*, 1263−1269.
(41) Thompson, J. D.; Gibson, T. J.; Plewniak, F.; Jeanmougin, F.; Higgins, D. G. The CLUSTAL_X Windows Interface: Flexible Strategies for Multiple Sequence Alignment Aided by Quality Analysis Tools. *Nucleic Acids Res.* **1997**, *25*, 4876−4882.
(42) Terp, G. E.; Christensen, I. T.; Jørgensen, F. S. Structural Differences of Matrix Metalloproteinases. Homology Modeling and Energy Minimization of Enzyme−Substrate Complexes. *J. Biomol. Struct. Dyn.* **2000**, *17*, 933−946.
(43) Goodford, P. J. A Computational Procedure for Determining Energetically Favorable Binding Sites on Biologically Important Macromolecules. *J. Med. Chem.* **1985**, *28*, 849−857.
(44) Boobbyer, D. N. A.; Goodford, P. J.; McWhinnie, P. M.; Wade, R. C. New Hydrogen-Bond Potentials for Use in Determining Energetically Favorable Binding Sites on Molecules of Known Structure. *J. Med. Chem.* **1989**, *32*, 1083−1094.
(45) Wade, R. C.; Clark, K. J.; Goodford, P. J. Further Development of Hydrogen Bond Functions for Use in Determining Energetically Favorable Binding Sites on Molecules of Known Structure. 1. Ligand Probe Groups with the Ability To Form Two Hydrogen Bonds. *J. Med. Chem.* **1993**, *36*, 140−147.
(46) Wade, R. C.; Goodford, P. J. Further Development of Hydrogen Bond Functions for Use in Determining Energetically Favorable Binding Sites on Molecules of Known Structure. 2. Ligand Probe Groups with the Ability To Form More Than Two Hydrogen Bonds. *J. Med. Chem.* **1993**, *36*, 148−156.
(47) Goodford, P. Atom Movements During Drug−Receptor Interactions. In *Rational Molecular Design in Drug Research, Alfred Benzon Symposium 42*; Liljefors, T., Jørgensen, F. S., Krogsgaard-Larsen, P., Eds.; Munksgaard: Copenhagen, 1998.
(48) Netzel-Arnett, S.; Fields, G.; Birkedal-Hansen, H.; Van Wart, H. E. Sequence Specificities of Human Fibroblast and Neutrophil Collagenases. *J. Biol. Chem.* **1991**, *266*, 6747−6755.
(49) Netzel-Arnett, S.; Sang, Q.-X.; Moore, W. G. I.; Navre, M.; Birkedal-Hansen, H.; Van Wart, H. E. Comparative Sequence Specificities of Human 72- and 92-KDa Gelatinases (Type IV Collagenases) and PUMP (Matrilysin). *Biochemistry* **1993**, *32*, 6427−6432.
(50) Niedzwiecki, L.; Teahan, J.; Harrison, R. K.; Stein, R. L. Substrate Specificity of the Human Matrix Metalloproteinase Stromelysin and the Development of Continuous Fluorometric Assays. *Biochemistry* **1992**, *31*, 12618−12623.
(51) Robinson, R. P.; Laird, E. R.; Blake, J. F.; Bordner, J.; Donahue, K. M.; Lopresti-Morrow, L. L.; Mitchell, P. G.; Reese, M. R.; Reeves, L. M.; Stam, E. J.; Yocum, S. A. Structure-Based Design and Synthesis of a Potent Matrix Metalloproteinase-13 Inhibitor Based on a Pyrrolidinone Scaffold. *J. Med. Chem.* **2000**, *43*, 2293−2296.
(52) Chen, J. M.; Nelson, F. C.; Levin, J. I.; Mobilio, D.; Moy, F. J.; Nilakantan, R.; Zask, A.; Powers, R. Structure-Based Design of a Novel, Potent, and Selective Inhibitor for MMP13 Utilizing NMR Spectroscopy and Computer-Aided Molecular Design. *J. Am. Chem. Soc.* **2000**, *122*, 9648−9654.
(53) Beckett, R. P.; Davidson, A. H.; Drummond, A. H.; Huxley, P.; Whittaker, M. Recent Advances in Matrix Metalloproteinase Inhibitor Research. *Drug Des. Today* **1996**, *1*, 16−26.
(54) Levy, D. E.; Lapierre, F.; Liang, W.; Ye, W.; Lange, C. W.; Li, X.; Grobelny, D.; Casabonne, M.; Tyrrell, D.; Holme, K.; Nadzan, A.; Galardy, R. E. Matrix Metalloproteinase Inhibitors: A Structure−Activity Study. *J. Med. Chem.* **1998**, *41*, 199−223.
(55) Cheng, M.; De, B.; Pikul, S.; Almstead, N. G.; Natchus, M. G.; Anastasio, M. V.; McPhail, S. J.; Snider, C. E.; Taiwo, Y. O.; Chen, L.; Dunaway, C. M.; Gu, F.; Dowty, M. E.; Mieling, G. E.; Janusz, M. J.; Wang-Weigand, S. Design and Synthesis of Piperazine-Based Matrix Metalloproteinase Inhibitors. *J. Med. Chem.* **2000**, *43*, 369−380.
(56) Jacobsen, E. J.; Mitchell, M. A.; Hendges, S. K.; Belonga, K. L.; Skaletzky, L. L.; Stelzer, L. S.; Lindberg, T. J.; Fritzen, E. L.; Schostarez, H. J.; O'Sullivan, T. J.; Maggiora, L. L.; Stuchly, C. W.; Laborde, A. L.; Kubicek, M. F.; Poorman, R. A.; Beck, J. M.; Miller, H. R.; Petzold, G. L.; Scott, P. S.; Truesdell, S. E.; Wallace, T. L.; Wilks, J. W.; Fisher, C.; Goodman, L. V.; Kaytes, P. S.; Ledbetter, S. R.; Powers, E. A.; Vogeli, G.; Mott, J. E.; Trepod, C. M.; Staples, D. J.; Baldwin, E. T.; Finzel, B. C. Synthesis of a Series of Stromelysin-Selective Thiadiazole Urea Matrix Metalloproteinase Inhibitors. *J. Med. Chem.* **1999**, *42*, 1525−1536.

JM0109053